Phase diagram and physical properties of a waterless sodium bis(2-ethylhexylsulfosuccinate)-ethylbenzene-ethyleneglycol microemulsion: An insight into percolation

S. K. Mehta* and Kawaljit

Department of Chemistry, Panjab University, Chandigarh 160 014, India

(Received 27 September 2000; revised manuscript received 28 September 2001; published 11 January 2002)

Volumetric and transport studies have been carried out for the nonaqueous ternary microemulsion system containing sodium bis(2-ethylsulfosuccinate) aerosol-OT (AOT), ethylbenzene (EB), and ethyleneglycol (EG). The results obtained for the conductivity σ are presented over a wide range of volume fraction of dispersed phase ϕ and different molar concentration ratio $\omega = [EG]/[AOT] = 2-10$ at 30 °C and discussed in context of percolation theory. The variation of σ with respect to temperature ($T = 10-60$ °C) shows an increase in the conductance values but no percolation-type phenomenon is observed. The measurements of viscosity, density, and ultrasonic velocity have also been carried out to understand the behavior of this nonaqueous microemulsion system. The phase behavior of the microemulsion is sensitively dependent on the EG to AOT molar ratio. A simple structural model has been applied for the calculation of the various parameters, i.e., aggregation number (n), core radius (r_n), and surface number density of the surfactant molecule at interface (α_s).

I. INTRODUCTION

Much is known about reverse micelles solubilizing water [1–3]. However, many reactions that one might want to scale down to the microreactor scale occur in the nonaqueous polar solvents. Some nonaqueous, highly polar solvents used commonly in chemistry include acetonitrile, methanol, and *N,N*-dimethyl formamide (DMF). While these solvents always show miscibility gaps with nonpolar solvents [4], there have been no reports of reverse micelles, as defined above, created using these solvents as the polar phase. For many chemical reactions, water is not the solvent of the choice as the medium in which reaction occurs. An attractive alternative for reactions in restricted geometries would be to isolate solvents other than water inside the micelles. A common surfactant used to create reverse micelles is aerosol OT (AOT).
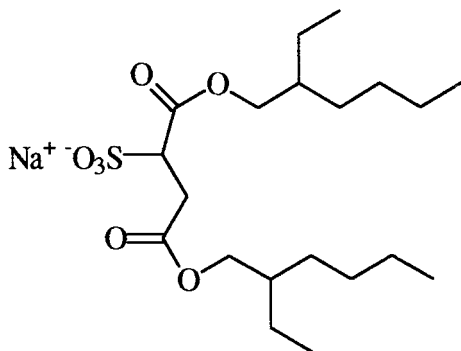
The characteristics of AOT reverse micelles in nonpolar solvents have been the focus of many studies [5]. AOT is used in particular because the micelles formed with this surfactant can solubilize a large quantity of water in a nonpolar solvent. While there are entire volumes describing micro-

emulsions of nonpolar solvents, water, and AOT, there exist only a few references to microemulsions where the polar phase is something other than water [6–17]. Polar solvents used include formamide, DMF, dimethylacetamide, ethyleneglycol, propylene glycol, and glycerol.

In continuation of our earlier work [18] and to obtain information on changes upon replacing water with ethylene glycol in the ternary system, the present work was undertaken. The study is expected to throw light on the interactions between surfactant and solvent other than water. The knowledge of such nonaqueous based microemulsions will give a better understanding of the creation of micellar environments and provides the framework for developing new chemical reaction media. Our present investigation includes systematic measurements of phase behavior, volumetric, and transport properties of nonaqueous microemulsions sodium bis(2-ethylhexylsulfosuccinate) (AOT)-ethylbenzene (EB)-ethyleneglycol (EG) throughout the single phase region at various ω (2–10). The analysis of the data will provide insight into the dynamics of clusters (percolation phenomenon) in nonaqueous systems.

II. EXPERIMENT

The nonaqueous microemulsions were prepared by mixing appropriate amount of AOT (Fluka), EB (E-Merck), and EG (Sisco research lab). AOT was purified in an active carbon/methanol slurry under stirring for 24 h. The sample was filtered and evaporated to dryness. The solidified AOT was further dried for 24 h in *vacuo* (0.05 mm Hg) at room temperature. It was immediately dissolved in nonaqueous polar component in the required ratio and was stored. EB and EG were used without further purification. A series of microemulsions were formed for different $\omega = 2-10$ and a dilution series of microemulsions were further studied by fixing ω but varying volume fraction in the range of $\phi = 0-0.545$. For AOT, critical micellar concentration [19] is of the order of $10^{-3}-10^{-4}$ mol dm^{-3} that is much lower than the concentration used in these experiments and therefore all the surfactant is considered to be localized at the interface. Assuming

―――――
*Author to whom correspondence should be addressed. Electronic address: skmehta@pu.ac.in
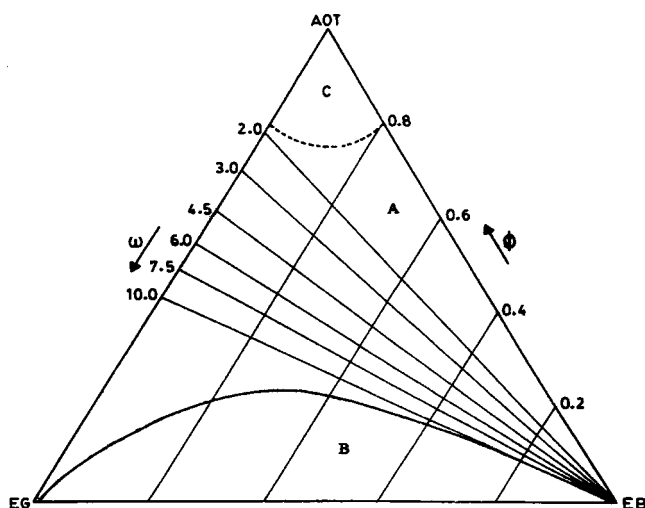
FIG. 1. Phase diagram of AOT-EB-EG microemulsion at 30 °C. *A*, single phase; *B*, double phase; *C*, mesophase.

negligible penetration of oil phase at the interface, the ϕ is defined as volume fraction occupied by the dispersed phase (AOT and EG) in the bulk organic phase.

$$\phi = \frac{V_{AOT} + V_{EG}}{V_{AOT} + V_{EG} + V_{EB}}$$

and

$$\omega = \text{molar concentration ratio} = [EG]/[AOT]$$

In the determination of phase diagram, the samples were equilibrated in a thermostated water bath maintained at 30 ± 0.1 °C. For each point in this phase diagram (Fig. 1), the composition of the three components is summed up in weight % composition and 100% composition was obtained.

$$X\% \ \ AOT + Y\% \ \ EB + Z\% \ \ EG = 100\% \quad (1)$$

Phase separation took place within few minutes but the samples were placed in water bath for hours/days to attain the proper equilibrium. The positions of these phase boundaries were reproducible.

The conductivities of the nonaqueous microemulsions were measured in thermostated glass cell with two platinum electrodes and digital conductivity bridge NDC 732 operating at 50 Hz from Naina electronics. The cell constant of the cell used was $1.0 \ \text{cm}^{-1}$. Measurement of conductivity was carried out with an absolute accuracy up to $\pm 3\%$.

Viscosity measurements were made using modified form of Ubbelholde's viscometer placed in a thermostated water bath. The estimated error in viscosity is less than 0.3%. The densities were measured with the help of ANTON-PAAR densimeter (DMA-60). The absolute uncertainty for density is estimated to be less than $10^{-5} \ \text{g cm}^{-3}$.

Ultrasonic time intervalometer was used for the precise measurements of ultrasonic velocities using pulse echo overlap technique. The principle of measurements is to make the two signals of interest overlap on the oscilloscope by driving the *X* axis with frequency whose period is the travel time

between the signals of interest. The precision in measured ultrasonic velocity values is $\pm 0.3\%$.

III. RESULTS AND DISCUSSION

A. Phase diagram

The ternary phase diagram for the nonaqueous AOT-EB-EG reverse microemulsion system at 30 °C is illustrated in Fig. 1. It is on the whole symmetrical and is sensitively dependent on the EG to surfactant molar ratio, i.e., ω. The Gibb's triangle shows comparatively a large one phase region (*A*) at low ω where microemulsion consist of nonaqueous droplets coated by surfactant monolayer dispersed in continuous medium of oil, i.e., microemulsion is formed that is in equilibrium with excess oil phase. Of the total triangular area, the monophasic area is estimated to be ~67%. A small two phase region (*B*) has been found at higher ω. At high concentration of emulsifier, i.e., at the top of the Gibb's triangle, the system is highly viscous that is due to mesophase *C*.

B. Transport properties

1. Conductivity measurements

Percolation and Scaling Laws. One expects various changes of the properties of the microemulsions, when the volume fraction of the dispersed phase (ϕ) is increased. The electrical conductivity should be especially sensitive to the aggregation of droplets. This is indeed observed in several reported studies [20–33] in aqueous microemulsions. The paper of 1978 by Lagues is the first to interpret the dramatic increase of the conductivity with droplet volume fraction for a water-in-oil microemulsion in terms of a percolation model and termed this physical situation as stirred percolation, referring to the Brownian motion of the medium. This was, however, soon followed by several investigations. According to most widely used theoretical model, which is based on the dynamic nature of the microemulsions [20–23,31–33], there are two pseudophases: one in which the charge is transported by the diffusion of the microemulsion globules and the other phase in which the change is conducted by diffusion of the charge carrier itself inside the reversed micelle clusters. According to this theory

$$\sigma = A(\phi_c - \phi)^{-s} \quad \text{where} \ \ \phi < \phi_c, \quad (2)$$

$$\sigma = B(\phi - \phi_c)^{t} \quad \text{where} \ \ \phi_c < \phi, \quad (3)$$

where σ is the electrical conductivity, ϕ is the volume fraction, and ϕ_c is the critical volume fraction of the conducting phase (percolation threshold) [28], and *A* and *B* are free parameters. These laws are only valid near percolation threshold (ϕ_c). It is impossible to use these laws at extremely small dilutions ($\phi \to 0$) or at limit concentration ($\phi \to 1$) and in the immediate vicinity of ϕ_c.

The validity of such laws for the nonaqueous microemulsions studied in the present work have been evaluated. Figure 2 shows the variation of conductivity (σ) as a function of volume fraction of dispersed phase (ϕ) for different ω
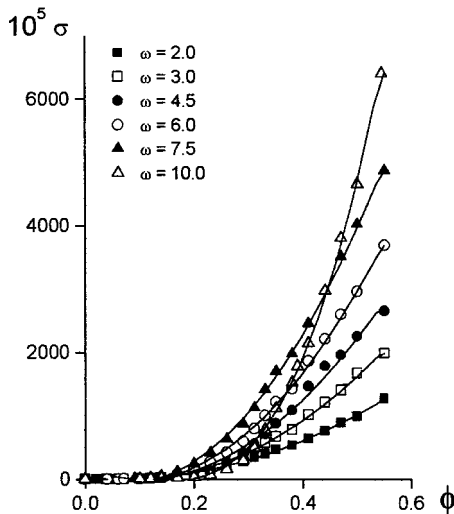
FIG. 2. Variation of conductivity $10^5 \sigma (\mathrm{Sm}^{-1})$ vs volume fraction ϕ for the system AOT-EB-EG at different ω.

FIG. 4. Variation of $d(\log_{10} \sigma)/d\phi$ vs ϕ for the system AOT-EB-EG at $\omega = 2.0$.

(2,3,4.5,6,7.5,10) at 30 °C. The conductivity of the system increases slightly at low ϕ but a sharp increase is observed at certain ϕ. This change has been attributed to the occurrence of percolation phenomenon. For our waterless system, by fitting the different values of s and t in Eqs. (2) and (3), the values of s and t obtained are 0.9 and 2.3, respectively. A good agreement between experimental and calculated values corresponds to Fig. 3 in which $(\sigma/A)^{-1/s}$ and $(\sigma/B)^{1/t}$ are plotted against ϕ. Moreover the resulting ϕ_c value is close to the value obtained by the numerical estimate of maximum of $d(\log_{10} \sigma)/d\phi$ vs ϕ (Fig. 4). Figure 5 also shows agreement between experimental and calculated values of $\log_{10} \sigma$ vs ϕ.

According to the static theory of percolation, the values of the critical exponents in the region above and below the threshold should be $t = 1.6$ and $s = 0.7$ [26,34,35]. However, because of the dynamic nature of the microemulsions, it has been theoretically and experimentally shown that both exponents should be higher than those predicted for static case [20–23,29–33]. Most of the s values reported for microemulsions are around 1.2 (in the range 0.7–1.6). The values of t are more scattered and is reported anywhere between
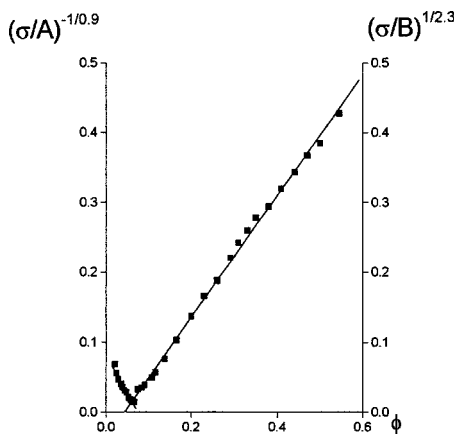
1.2–2.1 [36,37]. For the nonaqueous systems analyzed in this report, t is slightly above the range reported. It is important to note that the different experiments show the validity of percolation phenomenon independent of the nature of components (surfactant, oil, water or polar organic solvent) of the microemulsion or external fields (e.g., pressure) [38].

By increasing ω values, the magnitude of σ increases (Fig. 2). This may be due to the fact that with increase in ω, ionic strength decreases and spontaneous radius of the surfactant increases. The value of ϕ_c also increases with increase in ω (Fig. 6) which signifies decrease in attractive interactions between the droplets.

2. Temperature effect

The effect of change of temperature on the conductivity of AOT-EB-EG system has also been investigated in the temperature range ($T = 10$–60 °C) at constant $\phi \approx \phi_c$ and $\omega = 2$–10 as depicted in Fig. 7(a). With increase in the tem-

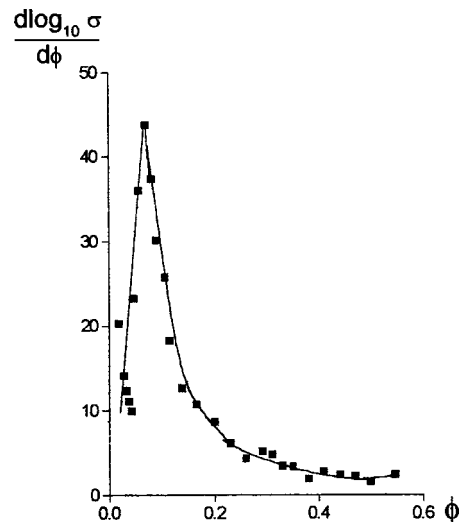FIG. 3. Variation of $(\sigma/A)^{-1/2}$ and $(\sigma/B)^{1/t}$ vs ϕ for the system AOT-EB-EG at $\omega = 2.0$.
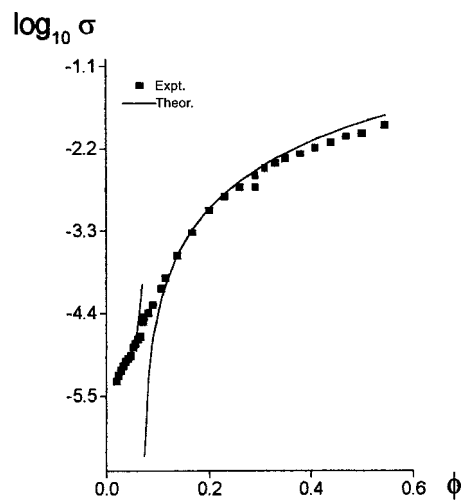

FIG. 5. Variation of $\log_{10} \sigma$ vs ϕ for the system AOT-EB-EG at $\omega = 2.0$.
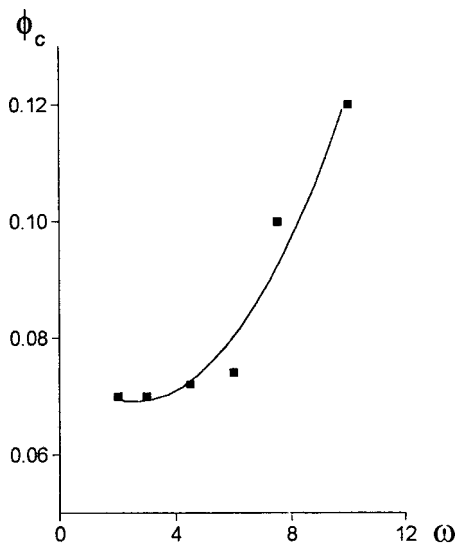
FIG. 6. Variation of percolation threshold ϕ_c vs molar ratio ω for the system AOT-EB-EG.

perature, conductivity of the system increases but no percolation-type phenomenon is observed. Figure 7(b) also shows the temperature effect at $\phi=0.31$ and $\omega=2-10$ of the system. Clearly, the system does not percolate with rise in temperature.

This is in line with the earlier observation by Alexandridis, Holzwarth, and Hatton [38] for aqueous based microemulsions. It was shown that for ω values less than or equal to 10, logarithm of conductivity increased linearly with temperature but did not suggest a percolation process. Because at low ω, conductivity is believed to originate from fluctuations in oil content of microemulsion droplets, such fluctuations result in charged droplets that can conduct electricity. An increase in temperature may increase the frequency of the charge fluctuations and thus increase in the conductivity.

Similarly, Peyrelasse and Boned [7] have shown that for the AOT-undecane-water system, the percolation occurs at $\omega=18$. Sagar, Sun, and Eicke [39] have studied conductivity vs temperature curves of AOT-hexane-water system at constant ω and ϕ. It has been shown that percolation occurs

within $(1.5<\omega<3.5)$ regime at higher ϕ: At $\omega=4.5$, the temperature dependent conductivity is little affected by ϕ. An AOT-decane-water microemulsion has been examined by Feldman *et al.* [40] at $\omega=26.3$ in an analysis of the mechanisms of charge transport above and below a conductivity percolation threshold induced by increasing temperature. More recent report by Alvarez *et al.* [41–44] on conductivity of AOT-isooctane-water system as a function of temperature and in the presence of various additives (ethyleneglycol, ureas, thioureas, amides, amines, and sodium salts) also shows the occurrence of percolation at higher value of ω $=22$ and 33.

3. Association model of droplet clustering

Various studies $[6-8,24,27-30,36-40,45-47]$ have shown that conductivity percolation in microemulsions is the result of droplet clustering. This is being depicted in Fig. 8. At low ϕ, individual droplets maintain a low conductivity. As ϕ increases, the conductivity also increases as droplets assemble in the clusters and ion diffusion or exchange of droplet content is facilitated and an infinite percolating droplet network is eventually formed at ϕ_c. Ray, Bisal, and Moulik [46] have estimated the energetics of the droplet clustering process utilizing the values of dispersed phase volume fraction (ϕ_c) at the percolation threshold. It has been postulated that the threshold of electrical percolation corresponds to the formation of first open structure of an infinite cluster [48,50,51]. The microemulsion droplet above the percolation threshold, aggregated in clusters, are considered to be phase different than that of nonpercolating droplets, with distinct physical properties such as conductivity. This is comparable to psuedophase concept used for modeling the formation of micelles in solutions of amphiphillic molecules (association model). Dilution of clustered (percolating) microemulsion system upon addition of an apolar solvent at constant droplet size lowers the conductivity rapidly until the clusters dissociate into individual droplets below percolation threshold ϕ_c; this phenomenon is comparable to the process of demicellization occurring when the surfactant concentration is lowered below the critical micellar concentration. In the light
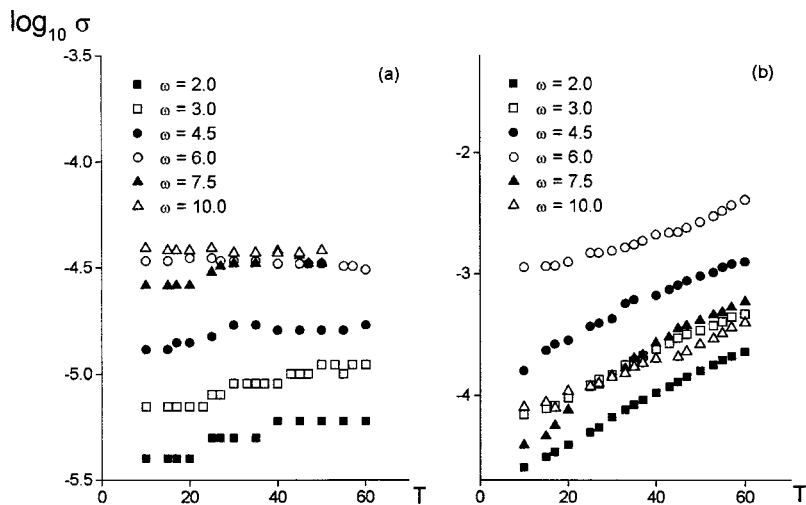

FIG. 7. Variation of $\log_{10}\sigma$ vs temperature T (°C) for the system AOT-EB-EG at different ω, (a) $\phi=\phi_c$; (b) $\phi=0.31$.
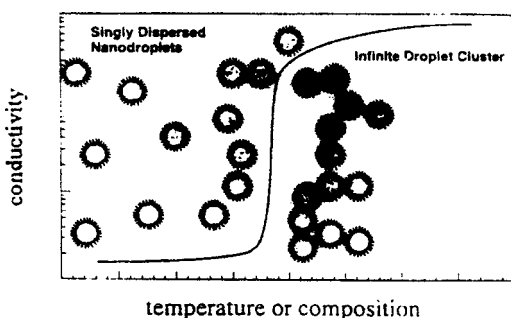
FIG. 8. Schematic representation of droplet cluster formation and the course of electric conductivity with varying temperature or composition without microemulsion.

of the concept of droplet association, the Gibb's free energy of droplet clustering (standard free energy change for the transfer of 1 mol of droplets from an infinitely diluted solution to the percolating cluster), ΔG_{cl}^{o} is calculated from the relationship

$$\Delta G_{cl}^{o} = RT \ln X_p \qquad (4)$$

where R is the gas law constant, T is the absolute temperature, X_p is the mole fraction of the microemulsion droplets corresponding to percolation threshold (ϕ_c) at constant temperature T and droplet size ω. The free energy of clustering, ΔG_{cl}^{o} values determined from X_p using Eq. (4) are shown in Table I. ΔG_{cl}^{o} is negative, since the droplet clusters are formed spontaneously.

At a given temperature, the value of free energy becomes less negative with increase in ω, showing that smaller the ω, more favorable is the droplet clustering.

4. Viscosity results

The variation of viscosity with volume fraction of dispersed phase ϕ at constant ω and T is shown in Fig. 9. It is clear that similar to conductance, viscosity of the system also increases with increase in ϕ. The effect of change of molar ratio ω is only on the magnitude of the viscosity but the over all trend remains same. For these nonaqueous microemulsion systems, viscosity also shows percolation phenomenon and obeys percolation laws. However, the viscosity percolation theory [6–7,9] is far less developed than complex permittivity percolation theory. However, by analogy with the conductivity equations, we can write

TABLE I. The value of ϕ_c and ΔG_{cl}^{o} for AOT-EB-EG system at 30 °C at various ω.

ω	ϕ_c	$\Delta G_{cl}^{o}(\text{kJ mol}^{-1})$
2.0	0.07	-7.45
3.0	0.07	-7.01
4.5	0.072	-6.51
6.0	0.074	-6.16
7.5	0.10	-5.25
10.0	0.12	-4.58

FIG. 9. Variation of viscosity η (cP) vs volume fraction ϕ for the AOT-EB-EG system at different ω.

$$\eta = A'(\phi_c - \phi)^{-s'} \quad \text{if} \quad \phi < \phi_c, \qquad (5)$$

$$\eta = B'(\phi - \phi_c)^{t'} \quad \text{if} \quad \phi > \phi_c, \qquad (6)$$

in which s' and t' are the two positive exponents, η_1 and η_2 are the viscosities of nonaqueous component and oil, respectively. The Eqs. (5) and (6) are valid only if $\eta_2 / \eta_1 \ll 1$. This condition is fully satisfied by the nonaqueous systems where the viscosity of oil (η_2) is much smaller than the viscosity of NPC (η_1).

The variation of $1/\eta(d\eta/d\phi)$ vs ϕ shown in Fig. 10 presents a maximum that corresponds to the percolation threshold ϕ_c. For our waterless system, the resulting ϕ_c is close to the one obtained by the numerical estimate of the maximum
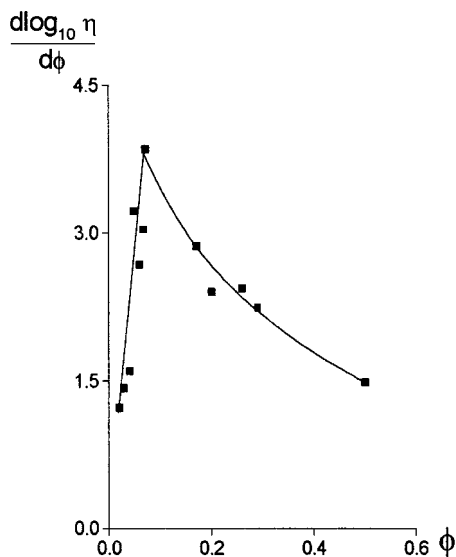

FIG. 10. Variation of $d(\log_{10}\eta)/d\phi$ vs ϕ for the system AOT-EB-EG at $\omega = 2.0$.
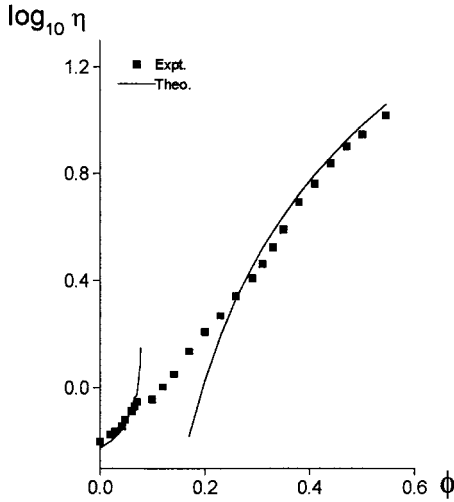
FIG. 11. Variation of $\log_{10} \eta$ vs ϕ for the system AOT-EB-EG at $\omega = 2.0$.

of $d(\log_{10} \sigma)/d\phi$ vs ϕ (Fig. 4). Figure 11 also shows good agreement between the experimental and calculated values of $\log_{10} \eta$ vs ϕ. By computational analysis of Eq. (5) and (6) the values of exponents s' and t' for the dynamic viscosity obtained are 0.2 and 1.8, respectively. Unexpectedly, s' has come out to be very small.

5. Analysis of relative viscosity (η_r)

In the dilute limit and for Newtonian behavior, η_r of a solution can be expressed by a virial-type [52] expansion in the volume fraction ϕ

$$\eta_r = \frac{\eta}{\eta_o} = 1 + A_1 \phi + A_2 \phi^2 + A_3 \phi^3 + \cdots, \qquad (7)$$

where contributions of ϕ^n order are due to effects involving at most n particles. In the very dilute limit, this virial equation reduces to well-known Einstein relation

$$\eta_r = \frac{\eta}{\eta_o} = 1 + 2.5\phi. \qquad (8)$$

According to this relation, the dispersed particles in the liquid are in the form of rigid spheres, which are larger than the solvent molecules. However, on account of complex interaction between the particles and solvent, the relation no longer remains linear when the concentration is increased ($\phi > 0.05$). Ward and Whitemore [53] have found that η_r is a function of size distribution and is independent of the viscosity of the suspending liquid and the absolute size of the spheres at a given concentration. According to Roscoe [54] and Brinkman [55], the viscosity of solutions and suspensions of finite concentration with spherical particles of equal size is given by

$$\eta_r = (1 - 1.35\phi)^{-2.5}. \qquad (9)$$

For large volume fractions one must, on the one hand, account for hydrodynamic interactions between the spheres

and on the other hand, for direct interactions between the particles that are, e.g., of a thermodynamic origin. For uncorrelated spheres the hydrodynamic interactions can be accounted for by formula derived by Saito [56,57]

$$\frac{\eta_r - 1}{\eta_r + 3/2} = \phi. \qquad (10)$$

However, the quantitative treatment of viscosity of microemulsions is not simple since one has to take into account various types of interactions. A variety of two parameter relations exist. In these relations, one parameter is connected with the effect of the isolated particles (Einstein coefficient) and the other with the interactions. Out of various types of equations using adjustable parameters, the most successful one is that of Mooney [58].

$$\eta_r = \exp\left(\frac{\alpha\phi}{1 - \lambda\phi} \right), \qquad (11)$$

where α is 2.5 when the particles are rigid spheres and no particle aggregates are present [59]. λ is the adjustable parameter known as crowding factor that takes care of particle interactions.

Another simple expression, which has been found to describe well the divergence of the relative viscosity at high concentration, has been given by Krieger [60]

$$\eta = \eta_o \left(1 - \frac{\phi}{\phi_p} \right)^{-1/v}, \qquad (12)$$

where η_o is the viscosity of the continuous phase, ϕ and ϕ_p are the volume fraction of dispersed phase and packing volume fraction at which viscosity diverges, respectively. ϕ_p and v are free parameters. The Krieger equation has been applied after estimating the values of ϕ_p and v by computational analysis. The value of ϕ_p for compact cubic arrangement of the spheres and for random arrangement of spheres is 0.75 and 0.65, respectively [61].

In Fig. 12, the experimentally determined viscosities from the microemulsions are represented as a function of dispersed phase volume fraction, ϕ. We compare these results with the data obtained from the Einstein, Brinkman, Saito, Mooney, and Krieger relations. As can be seen in Fig. 12, there is a good correlation between the experimental and theoretical data at lower concentrations ($\phi \approx 0.1$). At higher concentrations, the experimental data increases faster with concentration than is predicted by Einstein and Saito formulas, signifying that interactions are becoming important. The experimental η_r values deviate significantly from viscosities predicted by Brinkman equation. On the other hand, Mooney's equation predicts the experimental η_r reasonably well after estimating λ by computational analysis. With increase in ω, the magnitude of λ also increases (Table II) that signifies increased interactions between the particles. It has also been possible to fit η_r by Krieger equation when $\phi_p = 0.65$ and $v = 0.6$ at $\omega = 2$. The value of v decreases with increase in ω (Table II) whereas ϕ_p remains the same. A comparison of these computed parameters with the earlier studies on the
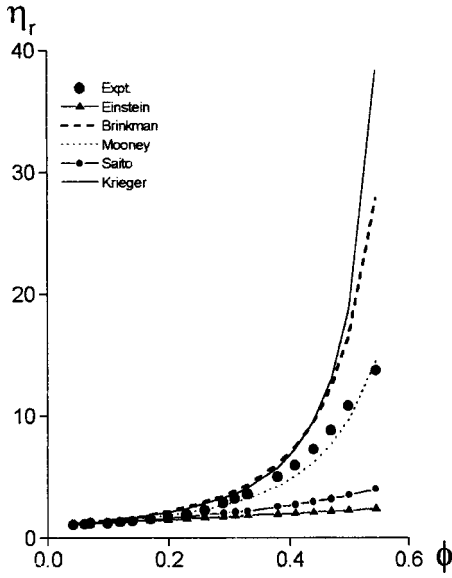
FIG. 12. Variation of relative viscosity η_r vs volume fraction ϕ for the system AOT-EB-EG at $\omega = 2.0$.

FIG. 13. Variation of ultrasonic velocity u (ms^{-1}) vs volume fraction ϕ for the AOT-EB-EG at various ω.

various systems shows a reasonable agreement, e.g., Abillon *et al.* [61] have obtained $\phi_p = 0.65$ and $\nu = 0.5$ for microemulsion comprising of CTAB-dodecane-brine-butanol, whereas values of 0.65 and 0.4, respectively, were evaluated by Cametti *et al.* [62] on a AOT-dodecane-water system. Leaver and Olsson [63] have used $\phi_p = 0.63$ and $\nu = 0.5$ for nonionic microemulsion comprised of $C_{12}E_5$-decane-water. Recently, Mehta and Kawaljit [64] have used value of ϕ_p and ν as 0.65 and 0.6, respectively for CTAB-alkanol-hydrocarbon-water system.

C. Volumetric properties

Volumetric properties, such as density and isentropic compressibility, provide useful information on the structural conditions of the micellar phase at different ϕ. The densities of these nonaqueous microemulsions for different $\omega = 2-10$ at $30\,°C$ show a linear trend. To account for the ϕ dependence on density and ultrasonic data, the role of micellar phase has been considered. Assuming the additivity of volumes of micellar and oil phases, the micellar density is calculated by using relation

$$\rho = \phi_m \rho_m + (1 - \phi_m) \rho_o, \tag{13}$$

TABLE II. The value of λ and ν at different ω for AOT-EB-EG microemulsion at $30\,°C$.

ω	λ	ν
2.0	0.90	0.60
3.0	1.00	0.60
4.5	1.20	0.50
6.0	1.30	0.45
7.5	1.35	0.40
10.0	1.35	0.40

where ρ_o and ϕ_m are the densities of oil and micellar phases, respectively. Equation (13) considers that the microemulsions are made up of two noninteracting regions, the micellar phase containing drops and bulk phase or oil phase [62,65]. Plots of $[\rho - (1 - \phi)\rho_o]$ vs ϕ for each ω show a linear trend, thus indicating the validity of Eq. (13).

A plot between ultrasonic velocity (u) and volume fraction of dispersed phase (ϕ) for different ω and constant T (Fig. 13) shows a decrease in u with increasing ϕ and then a sharp increase in u near $\phi = 0.12$. There is no evidence of discontinuity in ultrasonic velocity over the entire range. The change of ω cannot effect the trend of variation of u with ϕ, but it only effects the magnitude of u. To clarify the ultrasonic velocity behavior, the system is analyzed in terms of isentropic compressibility, that is more sensitive than velocity to structural changes. The isentropic compressibility (κ_s) is defined by

$$\kappa_s = -V^{-1}(\delta V/\delta \rho)_s, \tag{14}$$

where V is the volume of the mixture. The values of κ_s were calculated from u and ρ for the microemulsion using the relation

$$\kappa_s = 1/u^2 \rho, \tag{15}$$

which assumes that dissipative effects are negligible and that the hydrodynamic equation of motion can be linearized. The linear plot of isentropic compressibility vs volume fraction is consistent with the relationship

$$\kappa_S = \phi_m \kappa_{s,m} + (1 - \phi_m) \kappa_{s,o}, \tag{16}$$

where ϕ_m and ϕ_o are the volume fractions of the micellar and oil phase respectively. $\kappa_{s,m}$ and $\kappa_{s,o}$ are the isentropic compressibility of micellar phase and the isentropic compressibility of oil phase respectively. $\kappa_{s,m}$ and ρ_m calculated from above relations are plotted against ϕ in Figs. 14 and 15 respectively. From the figures, it is concluded that with in-
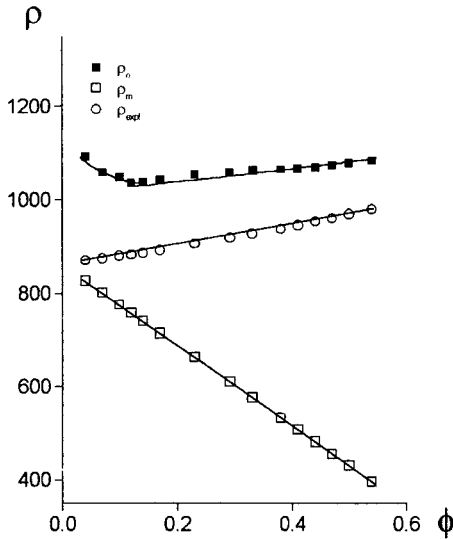
FIG. 14. Variation of density ρ (kg m^{-3}) vs volume fraction ϕ for the system AOT-EB-EG at $\omega = 2.0$.

crease in ϕ, ρ_m, and $\kappa_{s,m}$ decrease but the decrease is not very prominent, showing that the size of the particle is not dependent on ϕ.

D. Structural parameters

A simple structural model proposed by Casado *et al.* [49] has been utilized for computing the basic structural parameters, i.e., aggregation number (n), core radius (r_n), and surface number density of the surfactant molecules at the interface (α_s). In this model, a monodisperse population of spherical droplets of disperse phase, is considered to be separated from the organic phase by a monolayer of surfactant. The radius of the droplets is the sum of the radius of the nonaqueous core (r_n) and the length of the surfactant tails (l). The value of ϕ allows us to calculate the core radius (r_n)
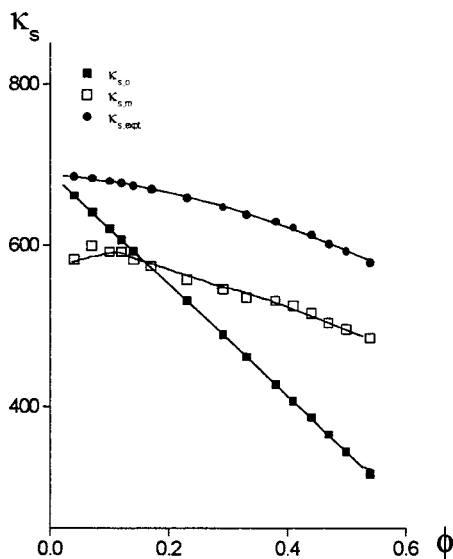

FIG. 15. Variation of isentropic compressibility κ_s (TPa^t) vs volume fraction ϕ for the system AOT-EB-EG at $\omega = 2.0$.

TABLE III. The value of n, r_n, and α_s at different ω for AOT-EB-EG microemulsion at 30 °C.

ω	n	r_n (nm)	α_s (nm^2)
2.0	88.86	1.51	2.82
3.0	135.57	2.08	2.48
4.5	219.78	2.80	2.22
6.0	321.25	3.50	2.09
7.5	439.25	4.18	1.99
10.0	674.83	5.31	1.90

and the aggregation number (n), which is the number of surfactant molecules per nonaqueous polar component droplet. Table III lists calculated value of n, r_n, and α_s using this model.

The systematic variation of ω has a well-defined effect on the structure of the droplets (Table III) and is represented in the form

$$r_n = 0.68(\pm 0.02) + 0.46(\pm 0.004)\omega. \quad (17)$$

There is now increasing evidence to suggest that the linear relationship is the result of various competing factors that conceal the underlying complexity of the structural changes.

The value of the interfacial area (a_{AOT}) per AOT molecule have also been calculated from the radius. For the AOT-EB-EG system the value of a_{AOT} obtained is 0.59 nm^2. The a_{AOT} value for AOT-EB-water is also estimated (0.52 nm^2) by the similar way. The two values are quite near to each other. It may be emphasized here that the model of particle system used in these calculations is very crude and ignores any possibility of polydispersity in the system. Therefore, it will be fitting to say that the similarity of the two systems is more significant than the minor difference revealed by the calculations.

IV. CONCLUSIONS

Nonaqueous ternary microemulsions of AOT of varying concentration and droplet size have been investigated in this work. The phase diagram has been delineated showing realm of existence of microemulsion region for the AOT-EB-EG system. It shows a large one phase ($\sim 67\%$) at low ω, a small double phase at high ω, and a mesophase towards the top of Gibb's triangle. The conductivity and viscosity of these systems, changes exponentially as the volume fraction of dispersed phase increases indicative of a percolation phenomenon. The variation of σ with respect to temperature T shows no sharp increase indicating that these systems do not percolate with increase in temperature. The free energy related to the cluster formation of microdroplet undergoing percolation is estimated using an associated model. The free energy of droplet clustering, i.e., ΔG_{cl}^o is negative since droplets assemble spontaneously in clusters. Viscosity results obey Einstein, Brinkman, and Saito relations only at low concentration whereas Mooney and Krieger equations fit the data in whole concentration range. The value of adjustable parameter λ increases and of ν decreases with increase in ω, which

signifies increased interactions between the particles. The calculated density of micelles (ρ_m) and isentropic compressibility of micelles ($k_{s,m}$) values decrease with ϕ but the decrease is not very prominent, thus one may conclude that the size of the particle is not dependent on ϕ. It is thus possible to obtain valuable information on the dynamics of nonaqueous microemulsion systems by the use of volumetric and transport properties.

[1] *Structure and Reactivity in Reverse Micelles*, edited by M. P. Pileni (Elsevier, Amsterdam, 1989), Vol. 65.

[2] *Reverse Micelles: Biological and Technological Relevance of Amphiphilic Structures in Apolar Media*, edited by P. L. Luisi and B. E. Straub (Plenum, New York, 1987).

[3] *Photochemistry in Microheterogeneous Systems*, edited by K. Kalyanasundaram (Academic, Orlando, FL, 1987).

[4] *Liquid-Liquid Equilibrium Data Collection I Binary Systems*, edited by J. M. Sørensen and W. Arlt (DECHEMA, Frankfurt, 1979), Vol. V, Part I.

[5] T. De and A. Maitra, Adv. Colloid Interface Sci. **59**, 95 (1995).

[6] J. Peyrelasse, C. Boned, and Z. Saidi, Prog. Colloid Polym. Sci. **79**, 263 (1989).

[7] J. Peyrelasse and C. Boned, Phys. Rev. A **41**, 938 (1990).

[8] C. Mathew, Z. Saidi, J. Peyrelasse, and C. Boned, Phys. Rev. A **43**, 873 (1991).

[9] Z. Saidi, C. Mathew, J. Peyrelasse, and C. Boned, Phys. Rev. A **42**, 872 (1990).

[10] S. Ray and S. P. Moulik, Langmuir **10**, 2511 (1994).

[11] R. E. Riter, J. R. Kimmel, E. P. Undiks, and N. E. Levinger, J. Phys. Chem. B **101**, 8292 (1997).

[12] K. Mukherjee, D. C. Mykherjee, and S. P. Moulik, J. Phys. Chem. **98**, 4713 (1994).

[13] S. E. Friberg, G. Rong, and A. J. I. Ward, J. Phys. Chem. **92**, 7247 (1988).

[14] M. Gautier, I. Rico, A. Ahmad-Zahed Samii, A. De Sangnac, and A. Lattes, J. Colloid Interface Sci. **112**, 484 (1986).

[15] E. Friberg and M. Podzimek, Colloid Polym. Sci. **262**, 252 (1984).

[16] Ahmad-Zahed Samii, A. De Savignac, I. Rico, and A. Lattes, Tetrahedron **41**, 3683 (1985).

[17] Y. A. Shchipunov and E. V. Shumilina, Colloid J. USSR **58**, 123 (1996).

[18] S. K. Mehta, Kawaljit, and Kiran Bala, Phys. Rev. E **59**, 4317 (1999).

[19] J. Peyrelasse and C. Boned, J. Phys. Chem. **89**, 370 (1985).

[20] M. Lagues, J. Phys. (France) Lett. **39**, L487 (1978); **40**, L331 (1979).

[21] M. Dvolaitzky, M. Guyot, M. Lagues, J. P. Le Plesant, R. Ober, C. Sauterey, and C. Taupin, J. Chem. Phys. **69**, 3279 (1978).

[22] M. Lagues, C. R. Acad. Sci. URSS **287**, 25 (1978); **288**, 339 (1979).

[23] M. Lagues and C. Sauterey, J. Phys. Chem. **84**, 1532 (1980); **84**, 3503 (1980).

[24] B. Lagourette, J. Peyrelasse, C. Boned, and M. Clausse, Nature (London) **5726**, 60 (1979).

[25] M. Moha-Ouchane, J. Peyrelasse, and C. Boned, Phys. Rev. A **35**, 3027 (1987).

[26] B. Antalek, A. J. Williams, J. Texter, Y. Feldman, and N. Garti, Colloids Surf., A **128**, 1 (1997).

[27] F. Caboi, G. Capuzzi, P. Baglioni, and M. Monduzzi, J. Phys. Chem. **101**, 10 205 (1997).

[28] M. S. Baptista and C. D. Tran, J. Phys. Chem. **101**, 4209 (1997).

[29] S. K. Mehta, R. K. Dewan, and Kiran Bala, Phys. Rev. E **50**, 4759 (1994).

[30] S. K. Mehta and Kiran Bala, Phys. Rev. E **51**, 5732 (1995).

[31] G. S. Grest, I. Webman, S. A. Safran, and A. L. R. Bug, Phys. Rev. A **33**, 2842 (1986).

[32] A. L. R. Bug, S. A. Safran, G. S. Grest, and I. Webman, Phys. Rev. Lett. **55**, 1896 (1985).

[33] S. A. Safran, I. Webman, and G. S. Grest, Phys. Rev. A **32**, 506 (1986).

[34] D. M. Grannan, J. C. Gailand, and D. B. Tanner, Phys. Rev. Lett. **46**, 375 (1981).

[35] Y. Song, T. W. Noh, S. I. Lee, and J. R. Gainis, Phys. Rev. B **33**, 904 (1986).

[36] S. Bhattacharya, J. P. Stokes, M. W. Kim, and J. S. Huang, Phys. Rev. Lett. **55**, 1884 (1985).

[37] M. G. Giri, M. Carla, C. M. C. Gambi, D. Senatra, A. Chittofrati, and A. Sanguineti, Phys. Rev. E **50**, 1313 (1994).

[38] P. Alexandridis, J. F. Holzwarth, and T. A. Hatton, J. Phys. Chem. **99**, 8222 (1995).

[39] W. Sager, W. Sun, and H.-F. Eicke, Prog. Colloid Polym. Sci. **89**, 284 (1992).

[40] Y. Feldman, N. Kozlovich, I. Nir, N. Garti, V. Archipov, Z. Idiyatullin, Y. Zuev, and V. Fedotov, J. Phys. Chem. **100**, 3745 (1996).

[41] E. Alvarez, L. García-Río, J. R. Leis, J. Mejuto, C. Juan, and J. M. Navaza, J. Chem. Eng. Data **43**, 123 (1998).

[42] E. Alvarez, L. García-Río, J. Mejuto, and J. M. Navaza, J. Chem. Eng. Data **43**, 433 (1998).

[43] E. Alvarez, L. Garcia-Rio, J. C. Mejuto, and J. M. Navaza, J. Chem. Eng. Data **43**, 519 (1998).

[44] E. Alvarez, L. Garcia-Rio, J. C. Mejuto, and J. M. Navaza, J. Chem. Eng. Data **44**, 484 (1999).

[45] J. Peyrelasse, M. Moha-Ouchane, and C. Boned, Phys. Rev. A **38**, 4155 (1988).

[46] S. Ray, S. R. Bisal, and S. P. Moulik, J. Chem. Soc., Faraday Trans. **89**, 3277 (1993).

[47] H. Mays, J. Phys. Chem. **101**, 10 271 (1997).

[48] H.-F. Eicke, M. Borkovec, and B. D. Gupta, J. Phys. Chem. **93**, 314 (1989).

[49] J. Casado, C. Izquierdo, S. Fuentes, and M. L. Moya, J. Chem. Educ. **71**, 446 (1994).

[50] *Organic Solvents: Physical Properties and Methods of Purification*, edited by J. A. Riddick and W. B. Bunger (Wiley Interscience, New York, 1970).

[51] A. D'Aprano, G. D'Arrigo, A. Paparelli, M. Goffredi, and V. T. Liveri, J. Phys. Chem. **97**, 3614 (1993).

[52] C. G. de Kruif, E. M. F. van Iersel, A. Vrij, and W. B. Russel,

J. Phys. Chem. **83**, 4717 (1985).

[53] S. G. Ward and R. L. Whitemore, Br. J. Appl. Phys. **1**, 286 (1950).

[54] R. B. Roscoe, J. Appl. Phys. **3**, 267 (1952).

[55] R. Brinkman, J. Chem. Phys. **20**, 571 (1952).

[56] N. Saito, J. Phys. Soc. Jpn. **5**, 4 (1950).

[57] N. Saito, J. Phys. Soc. Jpn. **7**, 447 (1952).

[58] M. Mooney, J. Colloid Sci. **6**, 162 (1951).

[59] S. Matsumoto and P. Sherman, J. Colloid Interface Sci. **30**, 525 (1969).

[60] M. Krieger, Adv. Colloid Interface Sci. **3**, 111 (1972).

[61] O. Abillon, B. P. Binks, C. Otero, D. Langevin, and R. Ober, J. Phys. Chem. **92**, 4411 (1988).

[62] C. Cametti, P. Codastefano, G. D'Arrigo, P. Tartagalia, J. Rouch, and S. H. Chen, Phys. Rev. A **42**, 3421 (1990).

[63] M. S. Leaver and U. Olsson, Langmuir **10**, 3449 (1994).

[64] S. K. Mehta and Kawaljit, Colloids Surf., A **136**, 35 (1998).

[65] G. D'Arrigo, A. Paparelli, A. D'Aprano, I. D. Donato, M. Goffredi, and V. T. Liveri, J. Phys. Chem. **93**, 8367 (1989).